**VTT Technical Research Centre of Finland**

# Lessons learnt - additive manufacturing of iron cobalt based soft magnetic materials

Lindroos, Tomi; Riipinen, Tuomas; Metsä-Kortelainen, Sini; Pippuri-Mäkeläinen, Jenni; Manninen, Aino

*Published in:*
Journal of Magnetism and Magnetic Materials

*DOI:*
10.1016/j.jmmm.2022.169977

Published: 01/12/2022

*Document Version*
Publisher's final version

Journal of Magnetism and Magnetic Materials 563 (2022) 169977

Contents lists available at ScienceDirect

Journal of Magnetism and Magnetic Materials

journal homepage: www.elsevier.com/locate/jmmm

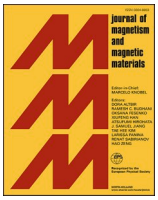

# Lessons learnt - additive manufacturing of iron cobalt based soft magnetic materials

Tomi Lindroos *, Tuomas Riipinen, Sini Metsä-Kortelainen, Jenni Pippuri-Mäkeläinen, Aino Manninen

*VTT Technical Research Centre of Finland Ltd., Kivimiehentie 3, Espoo 02044, Finland*

ARTICLE INFO

*Keywords:*
Soft Magnetic
Additive Manufacturing
Powder
Optimization

ABSTRACT

Additive manufacturing (AM) technologies have opened up new possibilities for realizing magnetic circuit designs, ultimately leading to electrical machines with enhanced performance, lower material consumption and cost. This study introduces lessons learnt of laser powder bed fusion (L-PBF) manufacturing of optimized soft magnetic cores. Processing routes from powder production of soft magnetic Fe-35Co, Fe-50Co, and Fe-49Co-2 V (Nb) materials, followed by process parameter optimization for L-PBF and finally the effect of heat treatment on the magnetic properties are shown. The major challenge is the mitigation of the eddy current losses. Effect of material composition as well as structural choices on the core losses of soft magnetic components are studied. Based on the magnetic measurements, the best heat treatment cycle led to magnetic saturation, permeability and coercivity comparable to commercial standardized Fe-49Co-2 V alloy. Magnetic measurement results of structurally modified test samples show that eddy current losses can be significantly reduced.

## 1. Introduction

Together with 3D design optimization, additive manufacturing (AM) provides unparalleled possibilities for creation of complex parts/components with improved characteristics. When it comes to the AM of electrical machinery, the soft magnetic cores present very interesting opportunities for weight savings and high-power densities. Garibaldi *et. al.* [1] was one of the first introducing studies about AM of Fe-Si based alloys, meanwhile Pippuri *et.al.* published the first results of optimized Fe-Co AM based components [2]. After that, the topic has received a great interest and the number of publications has been increased rapidly. Conducted studies are covering AM processing parameters optimization, alloys design and microstructure studies, and eventually 3D optimization of soft magnetic components, comprehensive reviews are given by Lamichhane *et.al* [3] and Pham *et.al.* [4].

In this work, we summarize the main findings on the laser powder bed fusion (L-PBF) of Fe-Co-based materials covering the pre-treatments, manufacturing, post-treatments as well as topological optimization (TO) of *meso*-structures to mitigate eddy currents.

## 2. Materials and methods

The Fe-Co alloy compositions studied cover Fe-35Co, Fe-50Co, Fe-49Co-2 V, and Fe-49Co-2 V(0.1Nb). The powder materials were gas atomized at VTT using a pilot scale Hermiga Gas Atomizing unit. Particle size distribution of the powders was classified suitable for L-PBF by sieving using 63 μm mesh sieve followed by particle size analysis using a Malvern laser diffraction. The powder morphology and flow properties were evaluated using Scanning Electron Microscopy and Hall-Flow test.

The parts were manufactured using SLM Solutions GmbH 125HL L-PBF machine equipped with 400 W IPG-YLR fiber laser in inert argon atmosphere while maintaining constant gas flow over the build platform. In the first stage the main L-PBF process parameters, i.e., laser power, hatch distance and scanning speed were optimized based on statistical Design of Experiment method. The printed test cubes were cut vertically and further ground and polished to get specimens for microscopy. Thresholded Optical Microscope (OM) images of the cross-sections were analyzed for porosity using ImageJ software. The process parameters that led to the lowest porosity were considered as the optimal parameters and further used to prepare samples including solids parts, e.g., bars and rings for characterization. Ring specimens with grooved and TO cross-section were designed and manufactured.

* Corresponding author.
*E-mail address:* tomi.lindroos@vtt.fi (T. Lindroos).

https://doi.org/10.1016/j.jmmm.2022.169977
Received 15 May 2022; Received in revised form 15 August 2022; Accepted 16 September 2022
Available online 21 September 2022

COMSOL multiphysics was used for TO of the ring sample cross-section targeting to minimize the eddy current losses and simultaneously maximize magnetic flux linkage in the secondary winding. The as-built samples were heat treated to control the microstructure of the studied materials and further the magnetic and mechanical properties. The effects of several different heat treatment cycles on evolution of the microstructure of samples of different sizes were studied.

For the ring samples quasi-static DC measurements were done up to 10 kA/m field strength and AC measurements in selected frequency and flux density operation points. The electrical resistivity of the bar samples was measured using four probes measurement method. The tensile tests were carried out at room temperature using Instron universal testing machine in accordance with ISO 6892–1 2016 standard. After optimization of each process step, the mechanical, magnetic, and electrical characteristics of the prepared samples were compared against commercial laminated (0.35 mm) alloy described in ASTM A801 standard.

## 3. Results and discussion

Several 5 kg batches were gas atomized to get the needed amount of the powders. All atomized powder batches showed similar particle morphology and particle size distribution after sieving. In the case of the Fe-50Co powder a bit higher amount of satellites was detected having a negative effect on the flowability. Average particle size distribution Dv50 for each alloy varied between 32 and 37 μm.

Threshold image analyses for porosity determination were done for Design of Experiment matrix consisting of 25 cube samples. Porosity values varied from 0.02 % to 0.53 %. The best laser parameters for the materials were: power = 200 W, scanning speed = 775 mm/s, hatch spacing = 80 μm. These parameters led to porosity level of below 0.1 % in all cases.

Optimized L-PBF parameters were used to produce samples for different characterization purposes, Fig. 1.

One of each sample type was left in as-built condition and the rest were heat treated to improve magnetic properties and to keep mechanical properties at acceptable level. Several different heat treatments were studied. One of the best heat treatment cycles consisted of pre-annealing at 700 °C for 2 h followed by anneal at 820 °C for 10 h. In comparison to anneal at 820 °C for 4 h, which is typically recommended to Fe-Co-V material, the difference in microstructures was drastic; conventional one step heat treatment led to bimodal type of grain growth whereas two stage cycle resulted in more equal large grain size structure, Fig. 2.

In the case of Fe-35Co and Fe-50Co alloys, the effect of different heat treatments was not so clear. In both alloys, the as-built microstructure consisted columnar grains growing parallel to the built direction. Changing from one stage to longer two stages heat treatment had only minor effect on the Fe-35Co microstructure, whereas both heat treatments caused some precipitation in Fe-50Co while grain size remained almost unchanged. In the case of binary alloys, the effect of these non-optimal microstructures can be seen in values of mechanical and magnetic properties. Both alloys were very brittle having in practice no measurable elongation in tensile test. Magnetic saturation values were high up to 2.40 T but were reached only with high magnetic field strengths when coercivity values varied from 735 to 1158 A/m, more detailed analysis is given in [5].

For ternary alloys Fe-49Co-2 V and Fe-49Co-2 V(0.1Nb), the importance of the optimized heat treatment is clearly seen. Non-optimal heat treatments led to bimodal grain growth and suppressed reaching good magnetic properties. Mechanical properties of the ternary alloys were not so sensitive for heat treatments and strength values comparable to reference alloy were achieved after optimized heat treatment [6], Table 1.

To get better understanding on the effect of the heat treatments and especially on the origin of the bimodal grain growth, series of heat treatments were done to samples with different size geometries. Heat treatments were done at 800 °C with holding times of 1 h, 10 h and 24 h. Due to differences in the thermal history during L-PBF processing, heat treatments caused different microstructures to small (10x10x35 $mm^3$) and to large (20x20x65 $mm^3$) samples. The most clearly this was seen in the case of 10 h holding time when microstructure of the larger specimen consisted of approx. 90 % large grains whereas smaller specimen had only 65 % larger grains. This effect can be clearly seen also in the magnetic behavior, Fig. 3. The larger size specimen consisting of almost totally larger grains reach high magnetic induction already at low magnetic field strength values whereas smaller size sample shows low permeability. After heat treatment with longer dwell time of 24 h, both specimen types had almost equal microstructures leading to good magnetic performance.

It is evident that size of the component leads to differences in thermal histories which is partially explaining the origin of bimodal type grain growth but cannot explain totally root cause for this behavior. Grain boundaries were studied by electron microscopy to find out possible impurities locking the grain growth. Some marks about oxides were detected but not clearly enough for the full explanation. In the case of 0.1 % Nb alloyed composition, less sensitivity to bimodal grain growth was detected. Nb is added in the standardized Fe-Co-V alloy to decrease grain growth. Similar behavior was detected in L-PBF samples when addition of 0.1 % Nb led approximately 50 % smaller grain size in as-built condition. Despite of the smaller grain size in as-built condition,

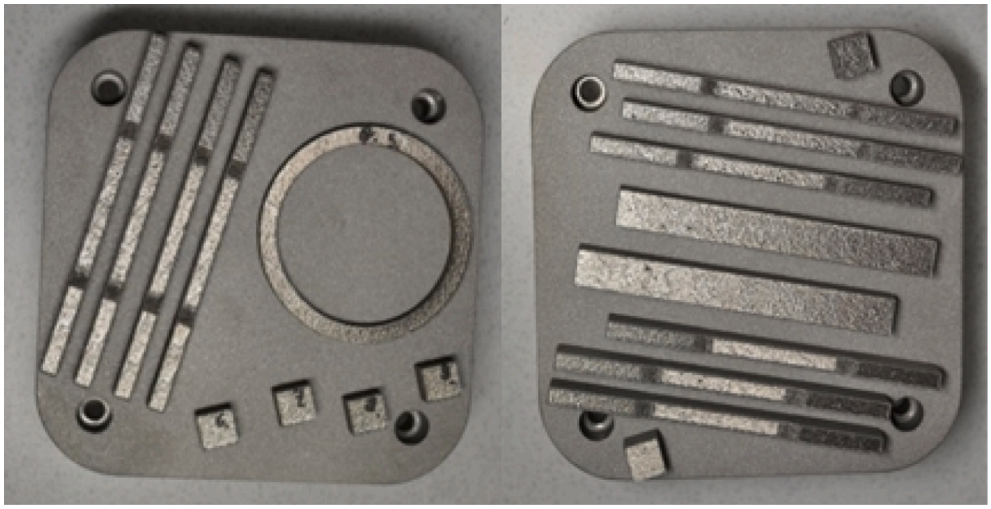

**Fig. 1.** Manufactured sample geometries: ring & bar samples for magnetic measurement, dog bone samples for mechanical testing and cubes for metallography.

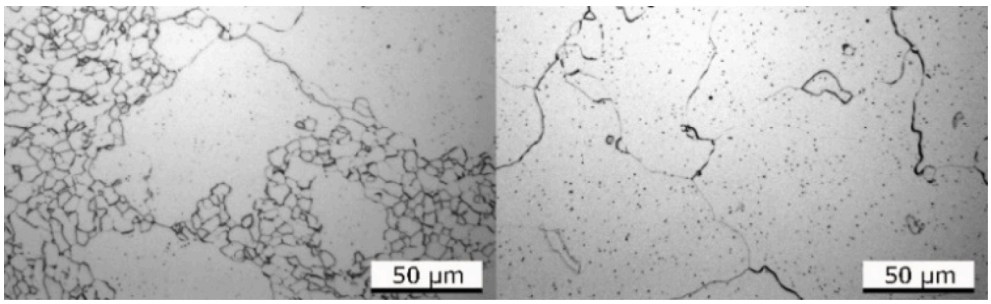


**Fig. 2.** Fe-49Co-2 V effect of the heat treatment on microstructure: left bimodal grain growth and right optimized large grain size.

**Table 1**
Magnetic, mechanical, and electrical properties of L-PBF Fe-49Co-2 V-(0.1Nb) (HT 700 °C/2h + 820 °C/10 h) compared to reference.

| | $H_c$ A/m | $B_{max}$ T | $\mu_{max}$ - | ρ µΩ m | $R_{0.2}$ MPa | $R_m$ MPa | A % |
|---|---|---|---|---|---|---|---|
| **L-PBF** | 47 | 2,23 | 13,000 | 47 | 266 | 306 | 3 |
| **Ref.** | 40 | 2,23 | 12,000 | 40 | 250 | 350 | 3 |

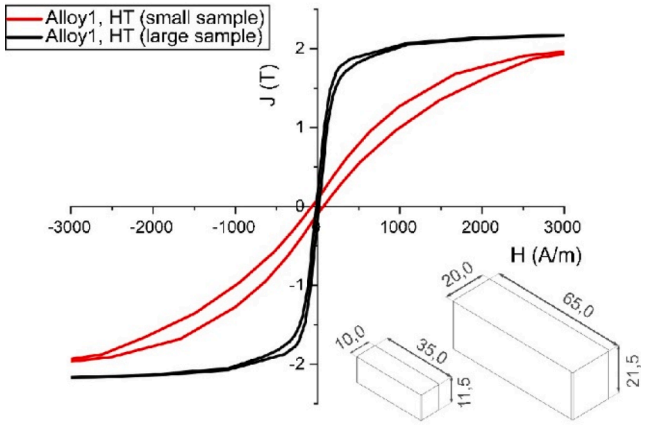


**Fig. 3.** Fe-49Co-2 V effect of test coupon size to grain size and further magnetic behavior after heat treatment 800 °C 10 h.

the grain size was growing more equally during heat treatments and finally, good magnetic properties were achieved also with shorter dwell times.

Mitigation of the losses can be approached practically in three different ways, by increasing electrical resistivity of the alloy, introducing *meso*-scale structures hindering eddy currents or by using multi-material structures consisting of electrically insulating layers. The current approach was based on both introducing alloy with moderate electrical resistivity and *meso*-scale structures. Alloying of binary Fe-Co alloy with V increased resistivity with ten folds to the value 49 µohm·m. meso-scale structures limiting eddy currents were studied in two ways by designing grooved structures and in a more advanced manner by using TO in the definition of the optimal cross-section for magnetic path. Examples of designed grooved and topology optimized specimens are shown in Fig. 4. Dimensions of the slits of the grooved structure were designed by modelling taking into account the limitations of the L-PBF process. Similarly, TO was used to minimize eddy currents and simultaneously maximize magnetic flux density. The most potential modelling results were used to realize ring shape test specimens for magnetic properties characterization.

Comparison of the magnetic response of each specimen type at DC and 50 Hz operation point is given in Fig. 5. In the case of DC, B-H curves of solid and laminated specimens are showing almost identical behavior

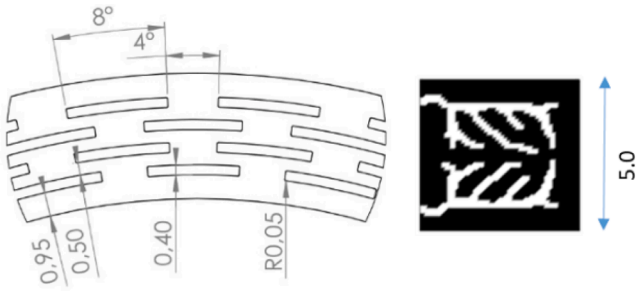


**Fig. 4.** Loss mitigating structures: Grooved structure consisting of small slits (left) and example about TO cross-section (right).

whereas grooved and TO specimens have deviation in the size and shape of the hysteresis loops. Coercivity values for grooved and TO specimens were 118 A/m and 74 A/m and permeability 5148 and 3489, respectively. By comparing these values to the values of solid and laminated specimens given in Table 1, a remarkable difference can be detected. This observation can be explained by size effect. Both grooved and TO specimens contain thin wall structures leading to different thermal history compared to the solid specimen. This results in similar behavior as presented in Fig. 3 for different size sample geometries.

Both grooved and TO specimens showed remarkable change in the shape and area of AC hysteresis loop compared to the solid specimen. Introducing slits to the grooved ring specimen offers a simple way to decrease eddy currents but still losses remain at rather high level. By using more sophisticated method, i.e., here TO for magnetic flux path cross-section design, eddy currents can be further decreased. In comparison to the laminated reference specimen, TO specimen shows similar coercivity values but permeability decreases at higher induction levels following shape of the DC B-H curve.

To compare power losses, the total losses of each specimen type were measured at 10, 50 and 100 Hz frequencies with 1.5 T magnetic induction. Power loss results of the solid, grooved and TO specimens were normalized with the value measured from laminated reference specimen, Fig. 6.

From normalized power loss values the effectiveness of the *meso*-scale eddy current mitigating structures is easily seen when excitation frequency is increasing. Rather simple grooved slit structure can decrease losses remarkably and more advanced topologically optimized structure leads to power losses comparable to the laminated reference structure.

It should be noticed that especially in the case of TO specimen, normalized losses are decreasing as a function of frequency. This is further confirming the role of quasi-static magnetic properties and microstructure. Based on this observation it can be expected to reach even lower power losses with TO specimen when microstructure corresponds to the microstructure and magnetic properties measured from solid specimens.

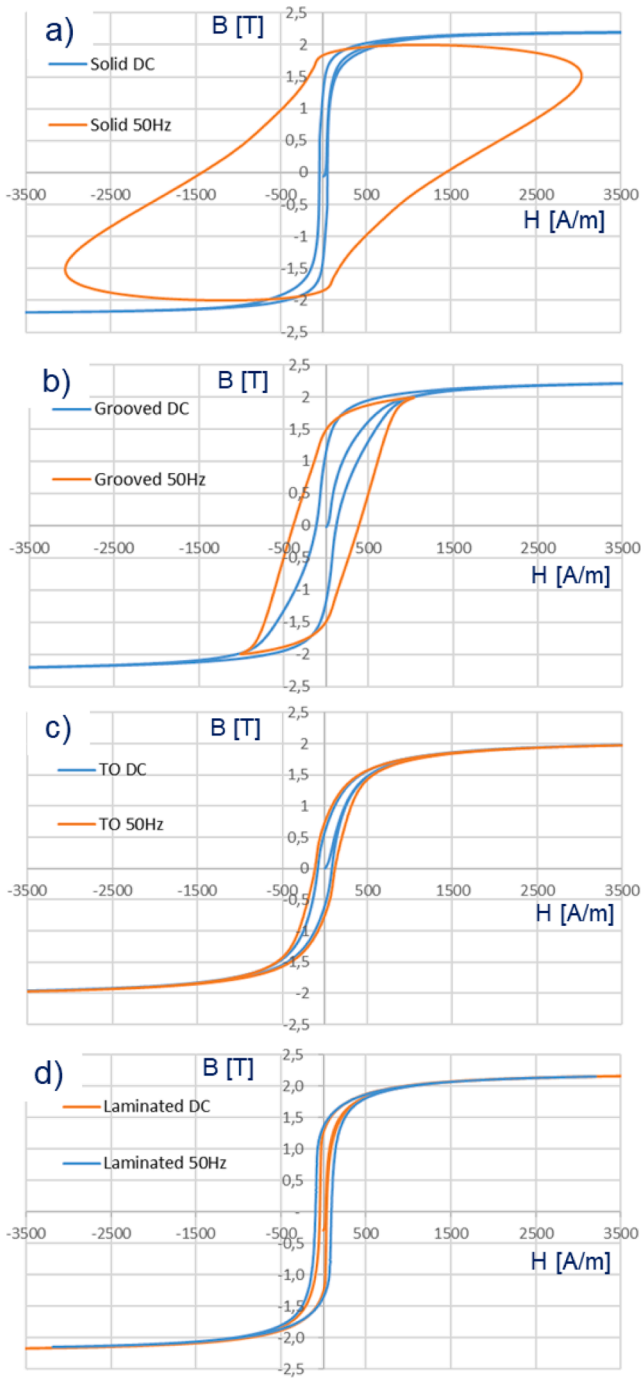


**Fig. 5.** Comparison of the measured DC and 50 Hz B-H curves a) solid, b) grooved, c) topology optimized and d) laminated reference.

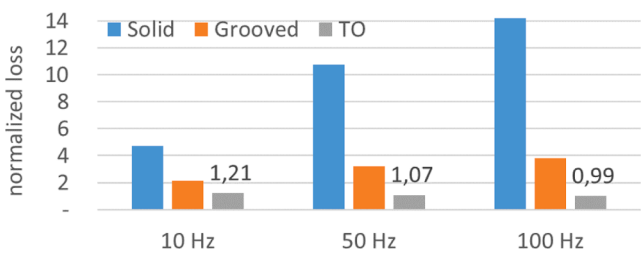


**Fig. 6.** Normalized losses of the solid, grooved and topology optimized specimens.

## 4. Conclusions

Processing routes from powder production to L-PBF manufactured test specimens for different Fe-Co based materials were conducted. Studies showed challenges to control brittleness and magnetic properties of the binary alloys. By alloying Fe-Co with V brittleness can be avoided, and further by adding 0.1 % of Nb, microstructure and that way also magnetic properties can be more precisely controlled. Importance of proper heat treatment was clearly shown. L-PBF components are having totally different as-built condition microstructure compared to standardized alloys which necessitates tailored heat treatment routes. Tendency for bimodal grain growth was detected which is partially explained with thermal history depending on the size of the component. With optimized processing parameters, magnetic properties comparable to standardized alloy were achieved. meso-scale structural optimization can be used to mitigate power losses also at higher frequencies. Losses comparable and even lower to laminated Fe-49Co-2 V reference were achieved with TO ring samples.

## CRediT authorship contribution statement

**Tomi Lindroos:** Conceptualization, Methodology, Validation, Formal analysis, Investigation, Data curation, Writing – original draft, Supervision, Project administration, Funding acquisition. **Tuomas Riipinen:** Conceptualization, Methodology, Validation, Formal analysis, Investigation, Data curation, Writing – review & editing, Visualization. **Sini Metsä-Kortelainen:** Conceptualization, Methodology, Validation, Formal analysis, Investigation, Data curation, Writing – review & editing, Supervision, Project administration, Funding acquisition. **Jenni Pippuri-Mäkeläinen:** Conceptualization, Methodology, Software, Validation, Formal analysis, Investigation, Data curation, Writing – review & editing, Supervision, Project administration, Funding acquisition. **Aino Manninen:** Conceptualization, Methodology, Software, Validation, Formal analysis, Investigation, Data curation, Writing – review & editing, Visualization.

## Declaration of Competing Interest

The authors declare that they have no known competing financial interests or personal relationships that could have appeared to influence the work reported in this paper.

## Data availability

Data will be made available on request.

## Acknowledgements

Academy of Finland funding 289338 & 306236 and VTT Technical Research Centre of Finland Ltd.

## References

[1] M. Garibaldi, I. Ashcroft, M. Simonelli, R. Hague, Metallurgy of high-silicon steel parts produced using selective laser melting, Acta Mater. 110 (2016) 207–216.
[2] J. Pippuri, et al., Manufacturing of Topology Optimized Soft Magnetic Core through 3D Printing, NAFEMS Helsinki, Finland, 2016.
[3] T.N. Lamichhane, L. Sethuraman, A. Dalagan, H. Wang, J. Keller, M. P. Paranthaman, "Additive manufacturing of soft magnets for electrical machines—a review", Materials Today Physics 15 (2020) 100255.
[4] T. Pham, P. Kwon, S. Foster, "Additive Manufacturing and Topology Optimization of Magnetic Materials for Electrical Machines – A Review", Energies 14 (2) (2021) 283.
[5] T. Lindroos, et.al., "Soft magnetic alloys for selective laser melting", EuroPM 2017 Congress and Exhibition.
[6] T. Riipinen, S. Metsä-Kortelainen, T. Lindroos, J.S. Keränen, A. Manninen, J. Pippuri-Mäkeläinen, Properties of soft magnetic Fe-Co-V alloy produced by laser powder bed fusion, Rapid Prototyp. J. 25 (4) (2019) 699–707.